

COMPARISON OF RESIDUAL SATURATIONS OF AN UNCONVENTIONAL RESERVOIR ROCK MEASURED BY DIFFERENT CAPILLARY PRESSURE LABORATORY METHODS

N. Schleifer⁽¹⁾, Alexandra Amann-Hildenbrand⁽²⁾, Jim Bell⁽³⁾, Philipp Aurin⁽¹⁾ and Roman Scheliga⁽²⁾

(1) Wintershall Holding GmbH, Central Laboratory, Germany; (2) RWTH Aachen, Institute of Geology and Geochemistry of Petroleum and Coal, Germany; (3) Advanced Rock Properties Group, Core Laboratories (U.K.) Ltd

This paper was prepared for presentation at the International Symposium of the Society of Core Analysts held in Vienna, Austria, 27 August – 1 September 2017

ABSTRACT

An extensive Special Core Analysis study was carried out on an unconventional gas reservoir from the Carboniferous sandstone. As the ambient porosity of the rocks is below 12 % and Klinkenberg corrected permeability is ranging in between 0.001 and 1 mD the laboratory study took almost two years. Saturation measurements were near the detection limit of all applied techniques while running the experiments following best practice procedures.

After finalizing the study the question arose whether such time consuming and cost expensive programs running at the limit of accuracy are appropriate for a proper reservoir characterization or whether a different “more easy” approach is required to deliver data, which would rather give trends and reduce measurement uncertainty by found statistics.

Accordingly a research program was started to compare the existing results with a different approach. Advanced core analysis capillary pressure methods as ultracentrifuge, porous plate and mercury injection (MICP) at overburden stress were compared to cost effective methods like ambient MICP, vapor desorption and adsorption as well as counter current imbibition (CCI) delivering a large amount of data, however at ambient conditions.

The paper shows the results of the different approaches under the consideration of accuracy and the governing physical principles/processes. However, their comparison is not straightforward as each method covers different pressure ranges and partially involve usage of non-reservoir fluids, which requires the transfer to representative wettability conditions. The results of this study show the advantages and disadvantages of characterizing such low porosity reservoir rocks and tries to define a complementary laboratory program delivering valuable results within acceptable time for a proper reservoir characterization.

INTRODUCTION

In 2012 about 130 m of core were taken from a Carboniferous tight gas reservoir in the Northern German Lower Saxony Basin. The six cored intervals cover a depth range from 3832.5m down to 4380.0m and comprise sediments from the Westphalian C to D or even Stephanian. The underlying Westphalian A-C coals are the origin of the accumulated gas. The sedimentological sequences of the reservoir mainly consist of thick sequences of fining upward fluvial sandstones which are separated by conglomerate and silty claystone units as well as anthracite coals. The gas-bearing fluvial sandstones have their origin in braided as well as meandering systems and were deposited in a broad alluvial plain in the northern forland basin of the Variscan mountain belt.

CORE ANALYSIS PROGRAM

A core logging and core analysis program was designed to characterize reservoir quality and rock mechanical behaviour. After running Routine Core Analysis on 230 fresh plugs a selection of 40 plugs was sent to CoreLab Aberdeen for Special Core Analysis. This program was finished in 2014. In 2015 a Master Thesis at RWTH Aachen (Scheliga, 2016) followed to apply complementary capillary pressure methods and to compare the results to the results generated by the SCAL program.

RESERVOIR ROCK CHARACTERIZATION

Core Analysis data shows that the reservoir quality varies in a narrow range. Ambient data give porosities below 12 % and Klinkenberg permeability between 0.001 and 1 mD. Based on this data a sedimentology and petrography study identified four main reservoir rock types (Table 1) where the main parts of RRT 3 and 4 are characterized by porosities below 5% and are commonly assigned to non-reservoir rock (Table 1).

Pore-throat-sizes (PSD) of all rock is below 1 μm (Fig. 1) with only a few samples showing macroporosity. X-ray diffraction analysis was carried out on all 40 SCAL plugs. Quartz and quartz cement content are between 54 and 90 wt.-%. Further abundant minerals are dolomite (1-18 wt.-%) and siderite (1-11 wt.-%). Clay minerals found are illite, mica, kaolinite and chlorite. The clay content varies between 11 and 29 wt.-%.

Thin section petrography by PanTerra Geoconsultants B.V. showed two diagenetic phases having an impact on the current porosity network. In a first stage the primary intergranular pore space was reduced by mechanical compaction and quartz cement precipitation during shallow burial. Secondary porosity was thereafter created by dissolution of feldspar under deep burial conditions. Illite and kaolinite formed due to feldspar dissolution, which filled the new pore space and reduced secondary porosity. Ductile grains were identified.

SAMPLE PREPARATION

Plugs of 1.5inch diameter are used for Routine and Special Core Analysis to maximize available pore volumes. Further 40 “twin”-plugs with 1 inch diameter were drilled for MICP at ambient and overburden conditions close to the SCAL plugs.

Plug cleaning for Special Core Analysis was done dependent on sample permeability. Lowest permeability samples were first saturated and immersed in 2 wt.-% KCl-brine while monitoring electrical conductivity. This should give an indication of the dissolution of precipitated salts in the pore space. The immersion cleaning of the samples indicated predominantly water wet behavior. Dependent on permeability increase samples were then either flow-through cleaned and or immersion cleaned in a Toluene-Methanol solvent mixture. No residual oil appeared while plug cleaning. Samples used in the Master Thesis were immersion cleaned in a mixture of iso-propyl alcohol and de-ionized water until no further dissolution of salt could be observed by measuring the electrical conductivity of the brine. Overall cleaning time took weeks to month.

LABORATORY METHODS APPLIED

The following methods (McPhee et al., 2015; Newsham et al. 2003 & 2004) were applied to measure capillary pressure and to define residual saturations for the static and dynamic reservoir model. Pore volumes vary between 0.25 mL and 5 mL. Given a measurement accuracy of 0.05 mL or 0.01g, partial saturations have an uncertainty of up to 20 %. Each method covers different pressure ranges and partially uses non-reservoir fluids (Table 2).

Porous Plate 1re Drainage Gas-Brine Pc at Reservoir Pressure

Porous plate measurements deliver a uniform fluid distribution while being able to run experiments at reservoir conditions and with reservoir fluids. As such no corrections need to be applied to consider overburden stress effects and wettability. Porous plate experiments are considered time consuming as sufficient time is required to achieve saturation stability. Porous Plate experiments are non-destructive.

Centrifuge 1re Drainage (Gas-Brine) and 1re Imbibition (Brine-Decane)

Ultracentrifuge runs are quick and achieve high capillary pressures. However viscous forces must be considered associated to the high spin speeds. As the capillary pressure varies along the plug axis centrifuge runs result in non-uniform fluid saturations which require a correction of the production data. This is regarded a source of error of the method. Running a gas-brine imbibition cycle requires to replace the gas phase by Decane to be able to monitor production and to ensure a proper displacement front.

MICP at overburden pressure (NOB 5000 psig)

The setup of mercury Pc measurements at overburden are comparable to porous plate Pc measurements. Mercury injection pressure is stepwise increased until mercury saturation becomes constant. As overburden pressure must be adjusted to the injection (pore) pressure to keep the net overburden pressure constant equilibration time to establish constant pressure conditions is a critical point. As the tests are run with two non-wetting fluids Pc curves must be corrected for interfacial tension and contact angles at reservoir conditions. Although reservoir wettability does not influence the experimental curve mercury displacing gas is considered an imbibition Pc curve.

MICP ambient

Commercial ambient mercury injection instruments were originally designed to measure pore throat size distributions of porous media. The benefit of these systems is that high P_c 's can be applied delivering a high amount of data-points. The benefit of these systems is that either small plugs or cuttings can be tested. Cuttings might require correction for surface roughness and porosity deviations to He-porosity. As with overburden experiments true wettability of the rock does not influence the experimental outcome. Ambient MICP systems allow the measurement of large samples series as analysis is quick and cheap.

Counter Current Imbibition (CCI)

CCI is cheap, easy to apply and allows quick analysis of large sample series. In this study Toluene was used as wetting fluid and gas the non-wetting phase. CCI does not apply a measurable capillary pressure. Toluene is spontaneously imbibed till end-point saturation is achieved. Initial saturation is set by evaporation (drainage). Confining pressure was not applied and whole sample surface was accessible to the wetting fluid.

Vapour desorption and adsorption

Vapour sorption curves are limited to high P_c 's and is dominated by the affinity of the pore surface to adsorb/desorb water vapour (physisorption). In comparison to proper P_c measurements saturation changes are not directly related to pore throat sizes. In this study desorption (drainage) and adsorption (imbibition) curves were measured in a climate chamber using a large sample group simultaneously. Saturation changes were monitored by weighting.

Capillary Pressure conversion

The conversion of the capillary pressure curves measured with different confining stresses and different fluid is based on the Leverett J-Function (1941),

$$P_{c1} = (\sigma_1 \cdot \cos \theta_1) / (\sigma_2 \cdot \cos \theta_2) \cdot P_{c2} \cdot \sqrt{(\Phi_1 / \Phi_2 \cdot K_2 / K_1)}, \text{ where} \quad (1)$$

P_{c1} indicates the references system, e.g. reservoir, and P_{c2} gives the capillary pressure to be converted, e.g. laboratory. Table 2 gives an overview of interfacial tension and contact angles of the rock-fluid systems. IFT at ambient conditions were measured by pendant drop method. Values for overburden measurements were taken from literature, e.g. McCaffrey (1972). A contact angle of 30° was assumed for the air-brine system.

EXPERIMENTS

Dry weight was recorded and the samples saturated either using a pressure of 2000 psig (CoreLab) or atmospheric pressure after initial vacuum period. Synthetic reservoir brine with a TDS = 211 g/L was used for porous plate and centrifuge testing.

Porous Plate 1^{re} Drainage (at 8700 psig overburden stress)

Porous plate measurements with a net confining stress of 8700 psi were part of the SCAL program. Method was performed on six samples using porous discs with a threshold pressure of 1500 psig. A maximum capillary pressure of 500 psig was applied.

Ultracentrifuge (ambient conditions)

Capillary pressure drainage and imbibition was measured by Ultracentrifuge within the SCAL program. No confining stress was applied. The drainage cycle was run using brine as the displaced fluid and air as the displacing fluid. The imbibition curve was run replacing air with decane as the displaced fluid. This is to avoid spontaneous brine imbibition during test loading. A maximum capillary pressure of 550 psig was applied. Capillary pressure curves were generated using Forbes equation (Forbes, 1994).

MICP at 5000 psig overburden stress

Five samples previously used for NMR testing were sent to Core Laboratories Houston for MICP curves at a net confining stress of 5000 psig. Maximum confining pressure of the setup allows 10 000 psi with a maximum mercury-air P_c of up to 5000 psia. Confining stress was continuously adjusted to keep net confining stress constant.

MICP at ambient conditions

Mercury injection capillary pressures (MICP) at ambient conditions were done with a Micromeritics® Autopore IV 9520™ porosimeter. Injection pressures up to 55 000 psi can be applied. In total 10 cylindrical samples of 1 inch diameter and 1 inch height were analyzed. Plug samples were hot solvent cleaned prior to testing.

Counter Current Imbibition (CCI) using Toluene at ambient conditions.

The experiments were run on 17 cleaned and dried samples (diameter 1.5 inch), saturated with toluene in a desiccator under vacuum conditions. Subsequently Toluene is evaporated at room temperature aiming for an initial target saturation of the plugs between 30 and 50 %. This range was defined by well-log interpretation. After setting initial saturation samples are wrapped with aluminum-foil and stored in a refrigerator at $T=4^{\circ}\text{C}$ for 24 h to keep the saturation constant and to achieve a homogeneous fluid distribution. Partially saturated sample were finally immersed in toluene and weight increase measured with an electronic balance. Imbibition was considered complete when no change of weight was observed within 0.5 h. Duration of one experiment was 15 to 20 hours. To avoid temperature variations all CCI experiments were run in a climate controlled laboratory room. CCI is a time- but no pressure controlled method; end-points saturations being determined are initial gas saturation S_{gi} and trapped gas saturation S_{gt} interpreted as residual gas saturation S_{gr} .

Vapour Desorption and Adsorption

Application of vapour sorption was adapted from soil science where relative humidity is set by using supersaturated brines. Core analysis adapted the method to achieve low initial water saturations (Newsham et al., 2003). Pressure achieved (10 000 psi) can

commonly only measured with MICP. The application assumes that the vapour pressure in the pores is in equilibrium with the fluid pressure and thus can be regarded equivalent to a capillary pressure. A climate chamber is used where temperature and relative humidity can be set with an accuracy of 0.1 °C and 0.5% rH. Samples were saturated with 2 wt.-% KCl. The brine was selected to avoid clay swelling. Temperature was set to $T=35^{\circ}\text{C}$ to allow a wider humidity range. Starting at 85% rH humidity was decreased down to 65% rH using incremental steps of 5 to 10% rH. The weight of the samples was recorded twice a week. In case no weight changes appeared between two consecutive records humidity was changed. Adsorption started immediately after desorption by increasing relative humidity up to 90% rH. Duration of the entire cycle was 5 month.

CHANGES OF PORE SIZE DISTRIBUTION WITH CONFINING STRESS

In Figure 1 the pore size distributions measured by MICP with and without confining stress are compared. Nearby plugs of reservoir rock type 1 and reservoir rock type 2 with similar basic petrophysical properties are shown. Ambient pore throat sizes are below $1\ \mu\text{m}$ with a distinct peak at $0.4\ \mu\text{m}$ for RRT 1 and a dual porosity distribution for RRT 2 with peaks at 0.4 and $0.015\ \mu\text{m}$.

Applying confining pressure leads to a single peak at $0.12\ \mu\text{m}$ without any distinct secondary peak. At NOB pore size distribution of sample 41A varies between 0.02 and $0.4\ \mu\text{m}$. Sample 160A shows pore throat sizes starting from $0.5\ \mu\text{m}$. As injection pressure is limited to 5000 psi no information on pore throat sizes below $0.02\ \mu\text{m}$ can be given.

RESULTS AT AMBIENT CONDITIONS

Centrifuge, MICP, CCI and vapor de- and adsorption were applied under ambient conditions. Only two: ultracentrifuge and vapor sorption, cover drainage and imbibition cycle. MICP data are converted to air-brine system assuming a water wet system with a contact angle of 0° . IFT of the synthetic reservoir brine is $78\ \text{mN/m}$. Figure 2 shows a comparison of the capillary drainage curves using the samples 123 (UC), 135 (MICP) and 137 (VD). MICP threshold pressure is higher than with ultracentrifuge. At a P_c of 100 psig (PTR $0.2\ \mu\text{m}$) and $S_w=0.6$ curves are crossing leading to a lower S_{wi} at 550 psig with MICP compared to centrifuge P_c . This is a general observation when comparing these two methods. A sample set representing rock type 3 ($\Phi = 4\%$, $K_L = 0.01\ \text{mD}$) shows the same cross-over at 100 psig and a $S_w=0.92$. To bring both curves to an overlap different sets of converting parameters would be necessary for MICP. One before and one after the cross-over. VD curves are shifted to higher capillary pressures compared to MICP leading to higher S_w at identical P_c . Comparing samples of same permeability the initial water saturation increases with the method applied (Fig. 4): $S_{wi}(\text{VD}) \leq S_{wi}(\text{MICP A-B}) \leq S_{wi}(\text{CCI}) \leq S_{wi}(\text{UC})$.

RESULTS AT OVERBURDEN STRESS

Comparing Porous Plate P_c and MICP at overburden pressure gives differences in S_{wi} of up to 0.4 (Fig. 6 and 7). Converting the MICP curve to 8700 psi by reducing porosity and

permeability S_{wi} can only be slightly increased. The example in Figure 3 shows an increase of 0.05. As a contact angle of 0° is already selected the only increase in MICP A-B NOB can be achieved by increasing the IFT of 52 mN/m or to assume different compressibility behavior of the plug. The overburden P_c curves show a parallel decrease of S_{wi} with K_L . The S_{wi} decrease is steeper (Fig. 4.) compared to ambient methods.

INITIAL VESUS RESIDUAL GAS SATURATION

Correlating S_{gi} with S_{gr} (Fig. 5) the methods ultracentrifuge, CCI and vapor de- and adsorption can be compared. Ultracentrifuge delivers lowest S_{gi} ($0.2 < S_{gi} < 0.7$) and lowest S_{gr} ($S_{gr} < 0.4$). CCI covers an intermediate range as S_{gi} was experimentally set to 0.5 to 0.8. These starting saturations result in a S_{gr} between 0.2 to 0.55. VD gives an S_{gi} above 0.8 with adsorption leading to a S_{gr} between 0.5 up to 0.8. Linear trend lines for S_{gi} vs S_{gr} of the three methods differ (Fig. 5). Vapor shows the steepest increase of S_{gr} with S_{gi} followed by CCI and ultracentrifuge measurements. CCI shows the largest scatter of residual saturations. Distinct trends for rock types are not recognizable (Fig. 6).

DISCUSSION

Tight sandstone samples were investigated with porosities below 12%. At such low porosity levels, any experimental errors in the detection of the partial saturations has large impact on the results. This is especially true for measurements at overburden stress.

Ambient MICP versus ambient air-brine P_c

In Figure 4 it is shown that MICP curves partly overlap with air-brine capillary pressure curves. A more complex conversion of MICP curves dependent on pore size would be required. To do so, interfacial tension and contact angles at reservoir conditions must be known. A constant contact angle of 30° was assumed in this study.

Overburden MICP versus Porous Plate at Reservoir Pressure

Comparing overburden MICP curves with porous plate air-brine P_c curves at overburden stress differ significantly (Fig. 3). There are no reasonable air-brine wettability parameters that bring both curves to an overlap. One reason for the large offset of both curves might be a varying NOB while MICP. Maximum P_c is set to 5000 psi with a maximum applicable NOB of 10 000 psi. Proper adjustment of overburden stress is therefore needed to guarantee a constant NOB and assumes that pore size distribution stays constant throughout the experiment. Saturation equilibration may another reason and have large impact on ambient P_c curves which increases with decreasing permeability, e.g. Maas et al. (2016).

S_{wi} versus Klinkenberg permeability

Although MICP and A-B P_c show a large offset in S_{wi} both method show almost parallel trends of S_{wi} versus K_L . The trend achieved of the overburden methods shows a steeper increase of S_{wi} with K_L than achieved by applying ambient methods (Fig. 4). An extension of the trend observed with ambient methods can not be extended to reservoir conditions. Vapor desorption results in lowest S_{wi} as highest pressures up to 10 000 psi

are applied. Ambient MICP converted to air-brine system and CCI show an overlap in residual saturations. CCI values were adjusted to a S_{wi} between 0.2 to 0.5 as this is the saturation range found by log interpretation. Application of centrifuge leads to highest initial water saturations also overlapping with CCI data.

S_{gi} versus S_{gr}

Plotting S_{gr} versus $S_{gi}=1-S_{wi}$ (Holtz, 2003) further discriminates the methods. Equal to S_{wi} applying VD leads to highest S_{gr} (0.5 to 0.8), CCI delivers intermediate values ($0.2 < S_{gr} < 0.55$) and ultracentrifuge testing leads to lowest S_{gr} (< 0.4). These correlations lead to different trends between S_{gi} and S_{gr} which depends on the applied methods (Fig. 5 and 6). Centrifuge testing uses brine as wetting fluid representing one of the reservoir fluids. Water wet behaviour of the rock leads to highest S_{wi} and thus lowest S_{gi} . VD has its benefit in achieving very low S_{wi} but adsorption is limited to a narrow saturation range. Using a different complementary method for achieving S_{gr} would improve the benefit of VD. Saturations measured with CCI are scattered allowing the extension of the trend derived from UC to higher saturations or the trend derived from vapor towards lower saturations. Obtaining a trend within the saturation range of interest, CCI would have to be applied starting with a wider range of initial saturations.

CONCLUSION

- Although at the detection limit, ambient and overburden Pc methods can be applied on low porosity ($\Phi < 12\%$) tight sandstone reservoir rock.
- Logarithmic trend of $S_{wi}-K_L$ found with ambient Pc methods can not be extended to reservoir conditions.
- MICP curves need to be compared to A-B Pc data to achieve a reasonable conversion to the reservoir fluid systems.
- MICP NOB data can not be brought in agreement with A-B Pc measured at overburden stress.
- CCI method must be applied using a wide range of S_{gi} to derive a valid $S_{gi}-S_{gr}$ relation in the saturation range of interest.
- $S_{gi}-S_{gr}$ relations of the reservoir rock types are dependent on the applied methods.
- Vapor desorption as imbibition capillary pressure method is not recommended.

NOMENCLATURE

A-B, ABRI: Air-brine capillary pressure (combined with resistivity index RI)

CCI: Counter Current Imbibition

Φ : porosity

IFT: interfacial tension σ

K, K_a K_L : Permeability, Air permeability, Klinkenberg Permeability

MICP: Mercury Injection Capillary Pressure

NOB: net overburden pressure, net confining stress

Pc: Capillary Pressure

PSD: Pore throat size distribution

P_{sig} , p_{sia} : Pressure in psi relative to atmospheric pressure (g) and vacuum (a)

RRT: reservoir rock type
 RCA, SCAL: Routine and Special Core Analysis
 S_{gi} : initial gas saturation ($S_{gi} = 1 - S_{wi}$)
 S_{gr} , S_{gt} : residual gas saturation, trapped gas saturation
 S_w , S_{wi} : Water saturation, initial water saturation
 TDS: Total dissolved solids
 θ : contact angle
 UC: ultracentrifuge
 VD: Vapor desorption

ACKNOWLEDGEMENTS

We would like to thank Wintershall Holding GmbH for the opportunity to present the data and to fund this study. Many thanks to all colleagues supporting the project.

REFERENCES

1. *Forbes P.L. (1994): Simple and Accurate Methods for Converting Centrifuge Data into Drainage and Imbibition Capillary Pressure Curves, The Log Analyst, 35/4, pp. 31-53.*
2. *Holtz, M. (2002): Residual Gas saturation to aquifer influx: A calculation method for 3-D computer reservoir model construction. SPE paper 75502. Society of Petroleum Engineers (SPE).*
3. *Leverett, M. C. (1941): Capillary Behavior in Porous Solids. Trans AMIE, 142, pp. 152–169*
4. *Maas, J.; Springer, N. and Hebing, A. (2016): Relative Permeability Effects Overlooked in MICP Measurements; Transition Zones Likely to be Smaller. Petrophysics, Vol.58, No. 1, pp. 19-27.*
5. *McCaffrey (1972): Measurement of interfacial tensions and contact angles at high temperature and pressure. Journal of Canadian Petroleum Technology, JCPT 72-03-03, July-Sept., pp. 26-32.*
6. *McPhee, C, Reed, J. and Zubizarreta, I. (2015): Core Analysis: A Best Practice Guide, Volume 64. Developments in Petroleum Science. Elsevier B. V., 1st ed.*
7. *Newsham, K.; Rushing, J. and Lasswell, P. (2003): Use of vapor desorption data to characterize high capillary pressures in a basin-centered gas accumulation with ultra-low connate water saturations. SPE paper 84596. Society of Petroleum Engineers (SPE).*
8. *Newsham, K.; Rushing, J.; Lasswell, P. and Blasingame, T. (2004): A comparative study of laboratory techniques for measuring capillary pressures in tight sands. SPE paper 89866.*
9. *Scheliga, R. (2016): Comparison of Capillary Pressure measurement methods applied to rock samples from a tight gas sandstone. Master Th. RWTH Aachen.*
10. *Suzanne, K.; Hamon, G and Billiotte, J. (2003): Experimental relationships between residual gas saturation and initial gas saturation in heterogeneous sandstone reservoirs. SPE paper 84038. Society of Petroleum Engineers (SPE).*

Table 1: Images and properties of representative rock type samples.

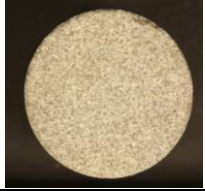
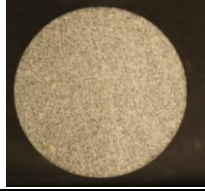
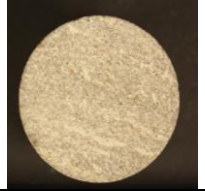
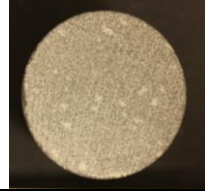
				
	RRT 1	RRT 2	RRT 3	RRT 4
Φ (fract.):	7 – 10	5–7	0–7	0–5
K_L (mD):	0.2-0.8	0.08-0.2	0.02-0.08	0.002-0.02
Grain density (g/mL):	2.65-2.67	2.67-2.71	2.70-2.78	2.70-2.78
Grain sizes:	Grain size tends to be medium to very coarse sand.	Medium sand grains	Grain size fine or medium sand.	Grain size fine or medium sand,
Deposit:	Braided channel deposits	Meandering to braided channel sediments.	Meandering channel to distal braided	Sheetflood sediments, very high content of ductile grains

Table 2: Overview of applied methods, capillary pressure ranges, fluid systems and fluid properties (* measure with pendant drop method).

Pc Method	Drainage (Swi)	Wetting Fluid	Non-wetting Fluid	IFT	Contact Angle
A- B Pc	x	Brine	Air	78	30
Centrifuge	x	Brine	Air	78	30
MICP @ NOB	x	Air	Brine	480	140
MICP amb.	x	Air	Brine	480	140
CCI					
Vapor	x	Brine	Air	72	30
Pc Method	Imbibition (Sgr)	Wetting Fluid	Non-wetting Fluid	IFT	Contact Angle
A-B Pc					
Centrifuge	x	Brine	Decane	50.6*	0
MICP @ NOB					
MICP amb.					
CCI	x	Toluene	Air	28.4*	0
Vapor	x	Brine	Air	72	30

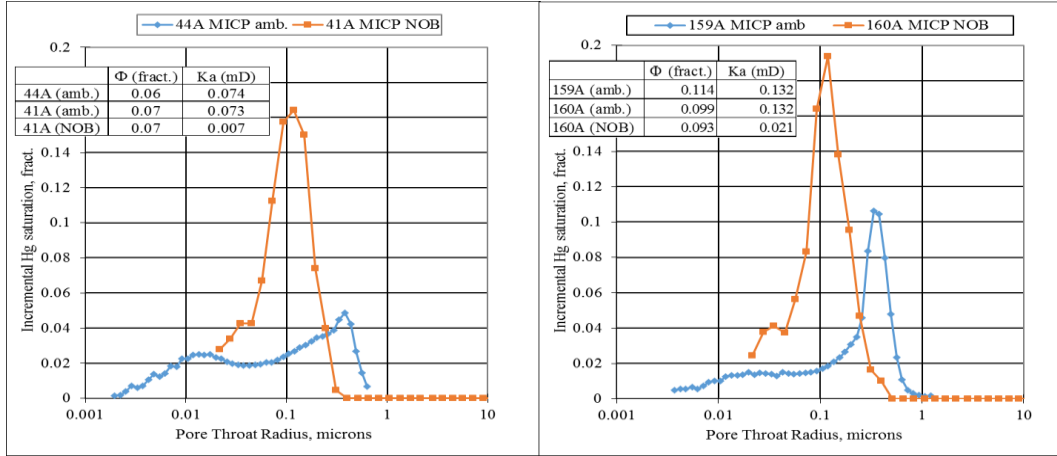


Figure 1: PSD at ambient and confining stress. Left: RRT 2. Right: RRT 1.

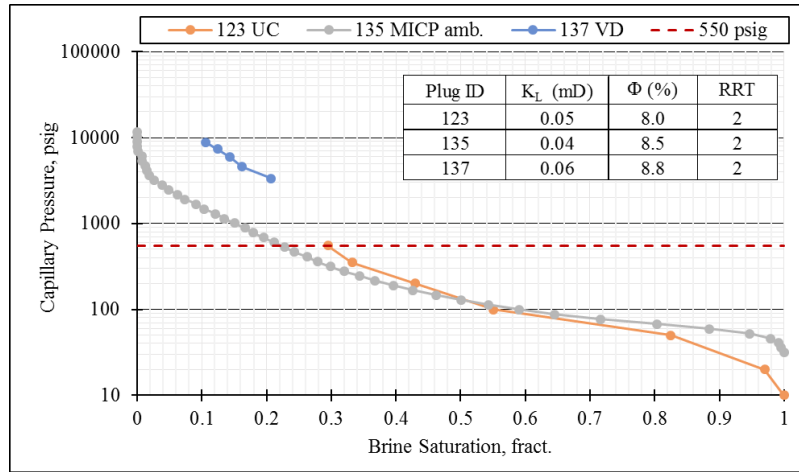


Figure 2: P_c from ultracentrifuge (UC), MICP ambient and vapor desorption (VD).

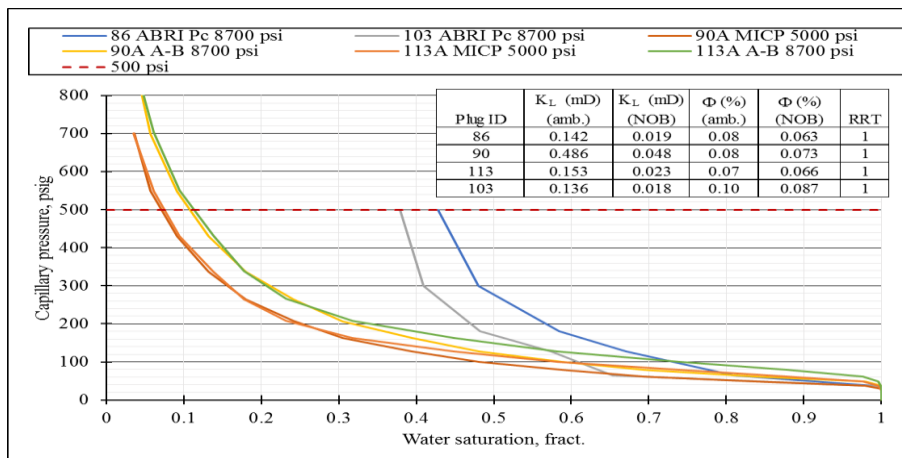


Figure 3: P_c curves from MICP NOB and porous plate (ABRI). Table in the graph gives petrophysical properties at measurement conditions and rock type of the samples.

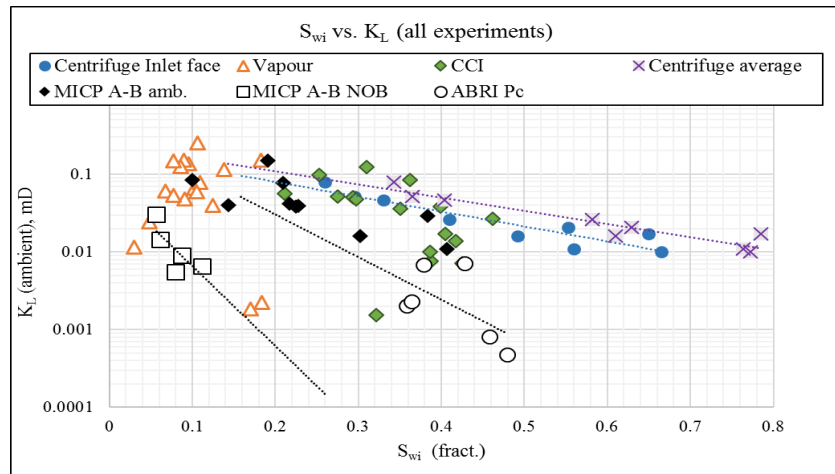


Figure 4: S_{wi} versus K_L (all experiments). MICP converted to A-B Pc and S_{wi} @ 500psig. Logarithmic trends are indicated.

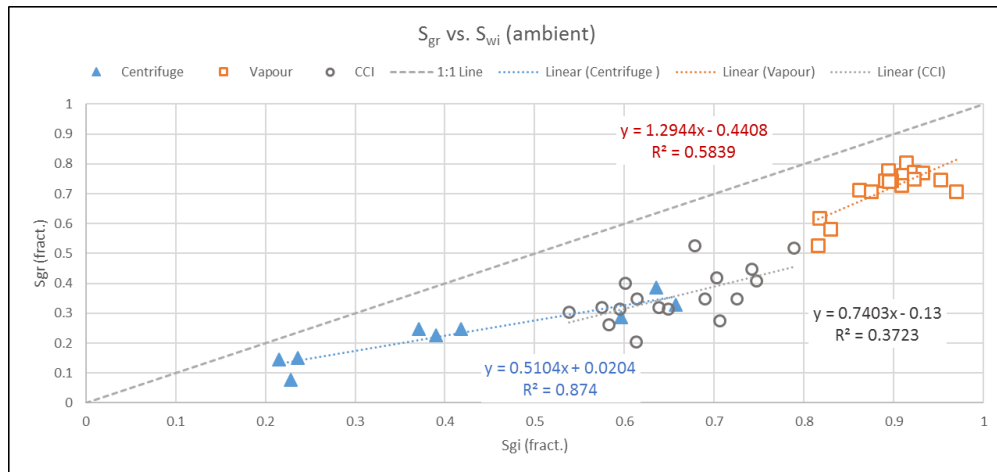


Figure 5: Initial gas saturations versus residual gas saturation sorted by experimental method.

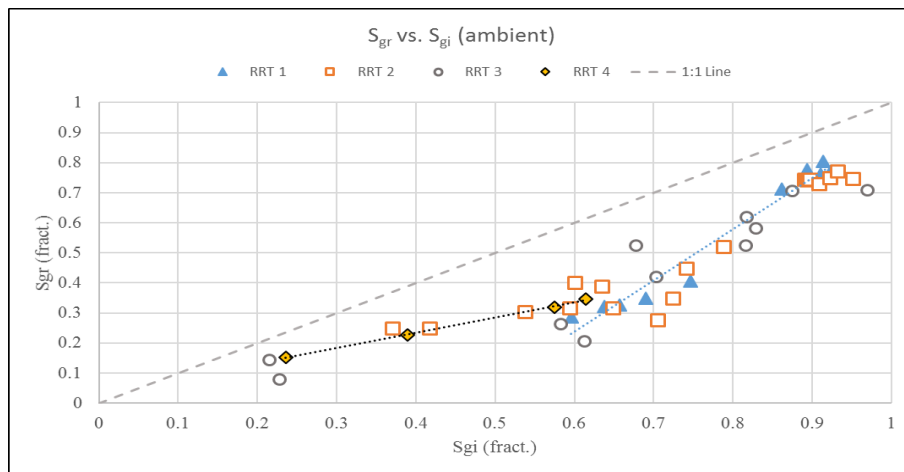


Figure 6: S_{gi} versus S_{gr} sorted by reservoir rock type (RRT).